

## Research Article

# Production of Reduced Graphene Oxide Platelets from Graphite Flakes Using the Fenton Reaction as an Alternative to Harmful Oxidizing Agents

Jean A. V. Piñas,<sup>1,2</sup> Tatiana S. Andrade,<sup>1</sup> Andreia T. Oliveira ,<sup>1</sup> Pedro E. A. Salomão,<sup>1</sup> Mariandry Rodriguez ,<sup>1</sup> Adilson C. Silva,<sup>3</sup> Henrique S. Oliveira,<sup>4</sup> Douglas S. Monteiro,<sup>1</sup> and Márcio C. Pereira <sup>1</sup>

<sup>1</sup>Institute of Science, Engineering, and Technology (ICET), Federal University of the Jequitinhonha and Mucuri Valleys (UFVJM), Campus Mucuri, Teófilo Otoni, 39803-371 Minas Gerais, Brazil

<sup>2</sup>Graduate Program in Biofuels, Federal University of Uberlândia (UFU), Uberlândia, 38400-902 Minas Gerais, Brazil

<sup>3</sup>Institute of Exact and Biological Sciences (ICEB), Federal University of Ouro Preto (UFOP), Ouro Preto, 35400-000 Minas Gerais, Brazil

<sup>4</sup>Department of Chemistry, Federal University of Minas Gerais, Belo Horizonte, 31270-901 Minas Gerais, Brazil

Correspondence should be addressed to Márcio C. Pereira; [mcpqui@gmail.com](mailto:mcpqui@gmail.com)

Received 16 August 2018; Revised 13 October 2018; Accepted 23 October 2018; Published 9 January 2019

Academic Editor: Vincenzo Baglio

Copyright © 2019 Jean A. V. Piñas et al. This is an open access article distributed under the Creative Commons Attribution License, which permits unrestricted use, distribution, and reproduction in any medium, provided the original work is properly cited.

The conventional chemical methods to produce graphene using strong oxidizing agents produce toxic gases during synthesis; therefore, these methods do not meet the principles of green chemistry. In this work, an alternative top-down method for the synthesis of a few layers of graphene sheets has been produced by a Fenton reaction- (a mixture of  $\text{Fe}^{2+}/\text{H}_2\text{O}_2$ ) assisted exfoliation process in water using graphite flakes as a starting material. Based on X-ray diffraction data and Fourier transform infrared (FTIR), Raman spectroscopy, and transmission electron microscopy measurements, it is proposed that the oxidation of graphite by Fenton chemistry facilitates the exfoliation of graphene sheets under mild sonication. Subsequent chemical reduction with ascorbic acid produced a few layers of reduced graphene oxide. Compared to Hummers' method, the Fenton reagent has similar exfoliation efficiency, but due to the Fenton reagent's preference to react with the edges of graphite, the chemical reduction can lead to the formation of less defective reduced graphene oxides. Moreover, since Fe and  $\text{H}_2\text{O}_2$  are cheap and environmentally innocuous, their use in large-scale graphene production is environmentally friendlier than conventional methods that use toxic oxidizing agents.

## 1. Introduction

Graphene is a two-dimensional (2D) graphitic structure which is the basic unit for making graphitic materials of other dimensionalities such as 0D fullerene, 1D carbon nanotube, or 3D graphite [1]. Because of its exceptional electronic, thermal, and mechanical properties [2–4], graphene has been investigated in several fields of science including catalysis

[5–7], adsorption [8–10], electrocatalysis [11, 12], energy storage [13–15], and sensors [16, 17].

Graphene is commonly synthesized by top-down methods using graphite as a precursor [18–26]. By this method, graphite is first converted into graphite oxide (GO) by strong oxidizing agents. This is generally exemplified by Hummers' method (a mixture of  $\text{KMnO}_4$ ,  $\text{NaNO}_3$ , and  $\text{H}_2\text{SO}_4$ ) [27] or modified Hummers' methods [28–31]. Dichromate and

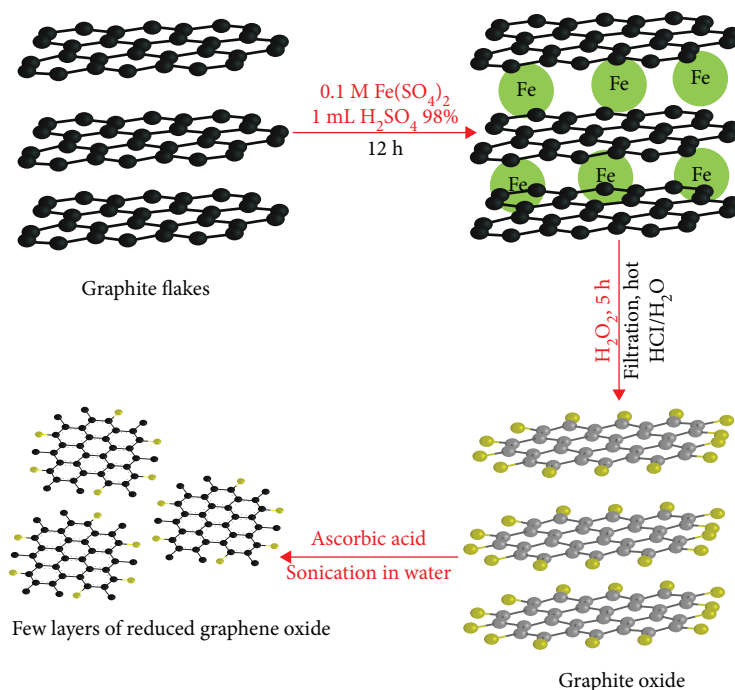


FIGURE 1: Steps for the preparation of a few layers of reduced graphene oxide from graphite flakes.

potassium chlorate in fuming nitric acid have also been used as oxidizing agents to produce GO [32, 33]. Then, GO can be converted into graphene oxide sheets by exfoliation and subsequently into graphene by reduction treatment using different methods such as thermal, chemical, or photocatalytic reduction [34–36].

The disadvantages of using conventional oxidizing agents for chemical exfoliation of graphite by Hummers' method or potassium chlorate is the generation of toxic gases such as  $\text{NO}_2$ ,  $\text{N}_2\text{O}_4$ , and  $\text{ClO}_2$ , which are profoundly harmful to the environment; therefore, they are unsuitable for large-scale green production of graphene. Recently, Agarwal et al. [37] reported a promising approach to produce a few layers of graphene by chemical exfoliation with Fenton chemistry. However, the use of organic solvent in the exfoliation process by sonication makes the process less green according to the principles of green chemistry [38].

In this work, we report an alternative aqueous route to prepare reduced graphene oxide (RGO) from graphite flakes using the Fenton reaction ( $\text{Fe}^{2+}/\text{H}_2\text{O}_2$ ) as an oxidizing agent. By this method, graphite is first oxidized by the Fenton reagent to produce graphite oxide. Then, graphite oxide is exfoliated by sonication and reduced by ascorbic acid to form RGO. Although the liquid waste from this synthesis contains  $\text{H}_2\text{SO}_4$ , the use of the Fenton reaction is attractive because Fe and  $\text{H}_2\text{O}_2$  are environmentally innocuous,  $\text{H}_2\text{O}_2$  activation takes place at room temperature and under atmospheric pressure, and the chemical reactions do not generate toxic gases. Moreover, the standard reduction potential of the  $\cdot\text{OH}$  radicals ( $E^\circ = 2.80\text{ V}$ ) is higher than those of permanganate ( $E^\circ = 1.51\text{ V}$ ) and dichromate ( $E^\circ = 1.33\text{ V}$ ), which are the most commonly used oxidizing agents for this purpose. Therefore, from a chemistry viewpoint, the graphene

sheets and their derivatives should also react with the hydroxyl radicals generated by the Fenton reaction.

## 2. Materials and Methods

**2.1. Material Synthesis.** Graphite oxide was prepared from expandable graphite (G), with an average flake size smaller than  $300\ \mu\text{m}$ , using a mixture of  $\text{Fe}^{2+}/\text{H}_2\text{O}_2$  as an oxidant. In short, 0.2500 g of graphite was mixed with 10 mL of 0.1 M  $\text{FeSO}_4 \cdot 7\text{H}_2\text{O}$  aqueous solution. Then, 1 mL of 98%  $\text{H}_2\text{SO}_4$  was added to the  $\text{Fe}^{2+}$ /graphite suspension, which was kept in an ice bath under constant stirring for 12 h. Then, 1 mL of 30%  $\text{H}_2\text{O}_2$  aqueous solution was added over about 5 h with constant stirring at room temperature. The solid was separated from the reaction mixture by filtration, washed several times with deionized water and hot  $\text{HCl}/\text{H}_2\text{O}_2$  to remove residual ions, and dried at room temperature. This sample was named GO(F). The resultant GO(F) was then readily resuspended in deionized water and sonicated at  $40^\circ\text{C}$  for 2 h. Then, the obtained suspension was centrifuged at 4000 rpm and the solid discarded to obtain a supernatant with a few layers of graphene oxide. The well-dispersed graphene oxide was finally reduced by ascorbic acid to form a few layers of reduced graphene oxide (RGO(F)). Subsequently, the mixture was centrifuged at 4000 rpm for 30 min to obtain a stable dispersion of RGO(F). The low-density material suspended at the top layer of the centrifuged solution was collected for further characterization. By this method, 0.3822 g of RGO(F) was produced from 0.2500 g of graphite. The steps for the RGO(F) preparation are shown in Figure 1. For comparison, the same procedure was repeated using Hummers' method to obtain reduced graphene oxide.

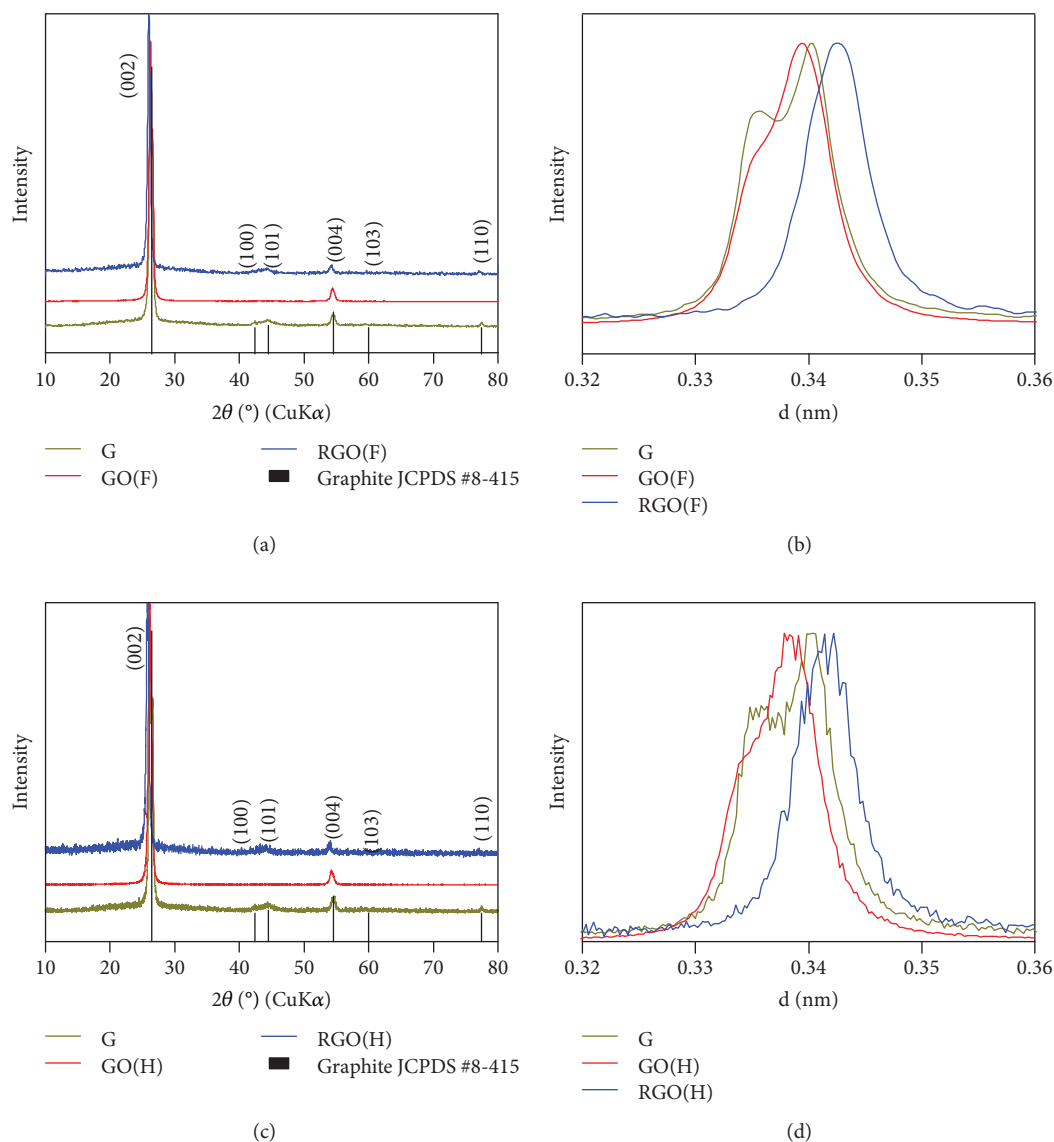


FIGURE 2: Powder XRD patterns and expanded XRD region for the (002) crystallographic plane of G, GO, and RGO samples obtained by (a, b) the Fenton method and (c, d) Hummers' method.

Hummers' method produced 0.3321 g of RGO(H) from 0.2500 g of graphite.

**2.2. Materials Characterization.** Powder X-ray diffraction (XRD) measurements were carried out at room temperature using a Rigaku Geigerflex diffractometer equipped with a graphite diffracted-beam monochromator. The data were collected in a  $2\theta$  range of  $10^\circ$  to  $70^\circ$  using Cu-K $\alpha$  radiation ( $\lambda = 1.5418 \text{ \AA}$ ), with an acceleration voltage of 40 kV, acceleration current of 20 mA, and scan speed of  $1^\circ/\text{min}$ . Fourier transform infrared (FTIR) spectra were obtained with a Nicolet 360 FTIR spectrometer equipped with a Smart OMNI sampler with a germanium crystal. Transmission electron microscopy (TEM) was performed on a JEOL JEM-2100F field emission transmission electron microscope with an accelerating voltage of 200 kV. The Raman spectra were obtained with a Senterra Raman microscope

spectrometer (Bruker, HR800 Labram I, Horiba Jobin Yvon) with an excitation wavelength of 633 nm. The samples were focused with a 100x lens, and the spectra were obtained using a 20 s integration time, five coadditions, and  $3.5 \text{ cm}^{-1}$  resolution. To prevent heat-induced phase changes via the excitation source while the Raman spectra were being collected, a line focus was utilized producing a line shape for the excitation source at the sample surface with a dimension of  $25 \times 1000 \mu\text{m}$  and using a laser power of 1 mW. Thermogravimetric analysis (TGA) was performed on a TG/DTA thermogravimetric analyzer (PerkinElmer Thermal Analysis).

### 3. Results and Discussion

The powder X-ray diffraction patterns of G, GO, and RGO synthesized by Fenton's and Hummers' methods are presented in Figure 2. The XRD data confirm the hexagonal

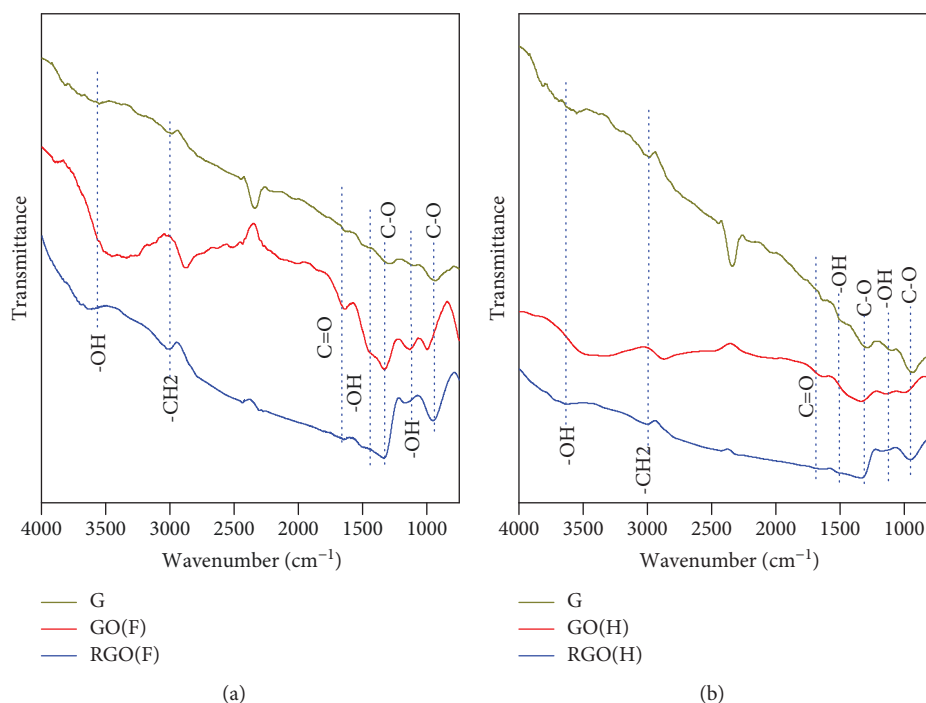


FIGURE 3: FTIR spectra of G, GO, and RGO samples obtained by (a) the Fenton method and (b) Hummers' method.

graphitic structure of the carbon materials according to the JCPDS # 8-415 (Figures 2(a) and 2(c)). It is worth noting that the XRD pattern of expandable graphite (G) exhibits a (002) basal plane with  $d_{002}$  spacing at 0.335 and 0.340 nm (Figure 2(b)), suggesting that the precursor had not expanded efficiently. The XRD pattern of sample GO(F) (Figures 2(a) and 2(b)) shows the 002 basal plane of graphite similar to that of sample G, except for the higher relative intensity ratio of  $d_{0.340}/d_{0.335}$  for sample GO(F) (1.7) compared to that of sample G (1.3), suggesting that the Fenton oxidation caused some structural defects in the graphene sheets of graphite [39–41]. Also, the oxidation of graphene sheets led to the disappearance of the (100), (101), and (110) planes in sample GO(F) due to the loss of  $sp^2$  carbon rings caused by the functionalization of the graphene sheets with oxygenated groups. The XRD pattern of sample RGO(F) shows that the (002) basal plane of graphite has shifted to the  $d$ -spacing value of 0.343 nm, while the (002) plane at  $d = 0.335$  nm utterly disappeared, suggesting a loss of the long-range order in graphene sheets due to the exfoliation process [39–41]. Notoriously, the (100), (101), and (110) planes were restored after the reduction of the oxidized graphene sheets by ascorbic acid, suggesting that the  $sp^2$  carbon rings have been restored. The XRD patterns of GO(H) and RGO(H) obtained by Hummers' method (Figures 2(c) and 2(d)) were quite similar to those obtained by the Fenton method. The (002) basal plane of graphite had shifted to a  $d$  spacing of 0.342 nm, which is close to the expansion of the graphene sheets obtained with the Fenton method.

The functional groups generated by Fenton oxidation of graphene sheets were evaluated by FTIR (Figure 3). The broad bands in the range of  $3600\text{--}3400\text{ cm}^{-1}$  are due to the vibrations of water molecules. The bands at around

$2995\text{ cm}^{-1}$  correspond to symmetric stretching vibrations of  $-\text{CH}_2$ . In the GO(F) and GO(H) sample, the band at  $2870\text{ cm}^{-1}$  is due to antisymmetric stretching vibrations of  $-\text{CH}_2$ . Intense bands at  $1660$  and  $1330\text{ cm}^{-1}$  are due to C=O and C-O stretching vibrations of the  $-\text{COOH}$  groups. These bands were more intense in the spectra of GO(F) and GO(H) samples, suggesting that graphite oxide is highly oxidized and consists mainly of  $-\text{OH}$  and other oxygenated functional groups. The intensities of the C=O, C-O, and  $-\text{OH}$  functional groups were greater in the GO(F) than in the GO(H) sample, indicating that the Fenton reaction was more effective in generating COOH and  $-\text{OH}$  in the graphene sheets of graphite than Hummers' reagent. Interestingly, the intensities of the C=O and  $-\text{OH}$  bands decreased after chemical reduction with ascorbic acid, indicating a partial removal of those functional groups to restore the  $sp^2$  carbon rings. Indeed, the reappearance of  $-\text{CH}_2$  groups at  $2995\text{ cm}^{-1}$  in the spectra of RGO(F) and RGO(H) confirms the restoration of  $sp^2$  carbon in the graphene sheets. Based on that, it is suggested that the C-O groups mainly occupy the basal planes while the  $-\text{COOH}$  and  $-\text{OH}$  groups are mostly found at the edges. Therefore, the C=O and  $-\text{OH}$  groups can be more easily reduced by ascorbic acid than the C-O groups.

The successful oxidation and exfoliation of graphite oxide were further verified by Raman spectroscopy. The Raman spectrum of carbon materials presents two main features, the D band at approximately  $1350\text{ cm}^{-1}$  and the G band at around  $1580\text{ cm}^{-1}$ . The D band is due to defect-mediated zone-edge phonons near the  $k$  point in the Brillouin zone, and the G band is due to the first-order scattering of the  $E_{2g}$  phonon of  $sp^2$  C atoms. Thus, the intensity ratio of the D and G bands ( $I_D/I_G$  ratio) can be used to estimate the number of defects in carbon materials. For an increasing

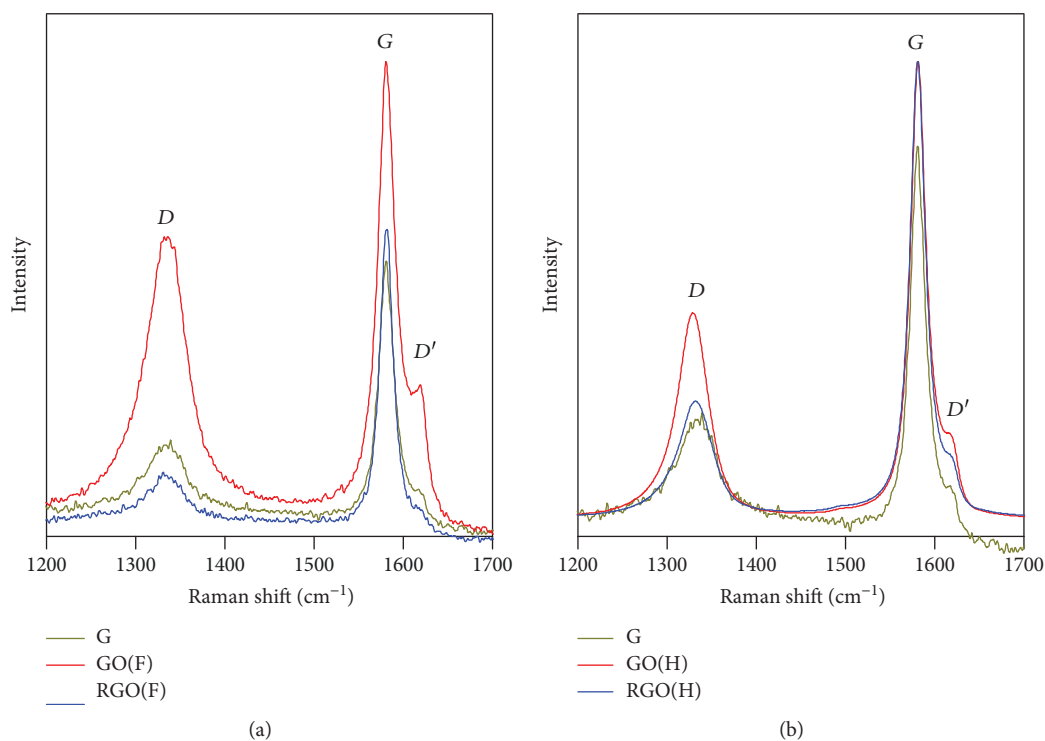


FIGURE 4: Raman spectra of samples G, GO, and RGO obtained by (a) the Fenton method and (b) Hummers' method.

number of defects,  $sp^2$  domains ( $G$  band) become smaller, and the intensity of the  $D$  band increases. Therefore, high  $I_D/I_G$  ratio values indicate the high functionalization degree of graphene sheets in carbon materials [42]. The Raman spectra of samples G, GO(F), and RGO(F) are shown in Figure 4(a). The spectra of all samples indicated two remarkable bands at around  $1336$  and  $1581$   $\text{cm}^{-1}$ , which correspond to the  $D$  and  $G$  bands, respectively. The  $I_D/I_G$  ratio for sample G (Figure 4(a)) was  $0.42$ , indicating that this graphite precursor is highly defective. After the oxidation of graphite by the Fenton reaction, the  $I_D/I_G$  ratio in sample GO increased significantly to  $0.64$ , suggesting the oxidation of graphene sheets in the graphitic structure, as also verified by FTIR. Hence, the Fenton chemistry can efficiently be used to weaken the van der Waals interactions of graphene layers, enabling the delamination of graphite by sonication. Indeed, the exfoliation/reduction of graphite oxide restores the  $sp^2$  network of graphene sheets and decreases the  $I_D/I_G$  ratio to  $0.21$ , suggesting that sample RGO(F) has less structural defects than its precursors. Furthermore, the  $D'$  band ( $1623$   $\text{cm}^{-1}$ ), usually reported for disordered graphitic lattices such as those introduced by heteroatoms, increases with the oxidation treatment and decreases upon the exfoliation/reduction procedure, confirming that RGO(F) has less structural defects than the G and GO samples. The error for the calculated  $I_D/I_G$  ratio is  $0.05$ .

For comparison, the graphite flakes were previously oxidized by Hummers' method followed by ultrasonication and reduction with ascorbic acid to produce reduced graphene oxide. The Raman spectra (Figure 4(b)) showed that the  $I_D/I_G$  intensity ratio of graphite oxidized (GO(H)) by Hummers' reagent was  $0.47$  while that obtained after

Fenton oxidation was  $0.64$ , suggesting that under the studied conditions the Fenton method was more efficient in oxidizing graphite than Hummers' method. After reduction, the  $I_D/I_G$  intensity ratio of RGO(H) decreased to  $0.28$ , while the reduction of RGO obtained by the Fenton method was  $0.21$ . It has been demonstrated that the Fenton reagent oxidizes the edges of graphite preferentially [37], and therefore, the reduction of graphite obtained from the Fenton route is more readily reduced than that obtained by Hummers' method.

Figures 5(a)–5(c) show the TEM images of samples G, GO(F), and RGO(F). Figures 5(a)–5(c) show that all the samples have the morphology of platelets. Figure 5(c) confirms that the Fenton oxidation favors the delamination of graphene layers from graphite by mild ultrasound. The EDX data for the RGO(F) (Figure 5(d)) present only signals of C, O, S, and Cu. S is due to the ferrous sulfate, and Cu is the support for the RGO. No signal of Fe was identified by EDX, suggesting that  $\text{HCl}/\text{H}_2\text{O}_2$  was efficient in completely removing iron from the graphene sheets. HRTEM analysis (Figure 5(e)) displays a close-to-ideal crystalline-reduced graphene oxide that consists of 6 layers with a  $d_{(002)}$  spacing of  $0.33$  nm. It was noted from Figure 5(f) that the previous Fenton oxidation of a graphite precursor is essential for obtaining a few layers of reduced graphene oxide. If the Fenton oxidation of graphite is not previously performed, an RGO with multiple layers is obtained. Figure 5(g) shows the morphology of the RGO(H) obtained by Hummers' method, which resulted in approximately 8 layers of reduced graphene oxide (Figure 5(h)), suggesting that the exfoliation by the Fenton method is comparable to that of Hummers' method.

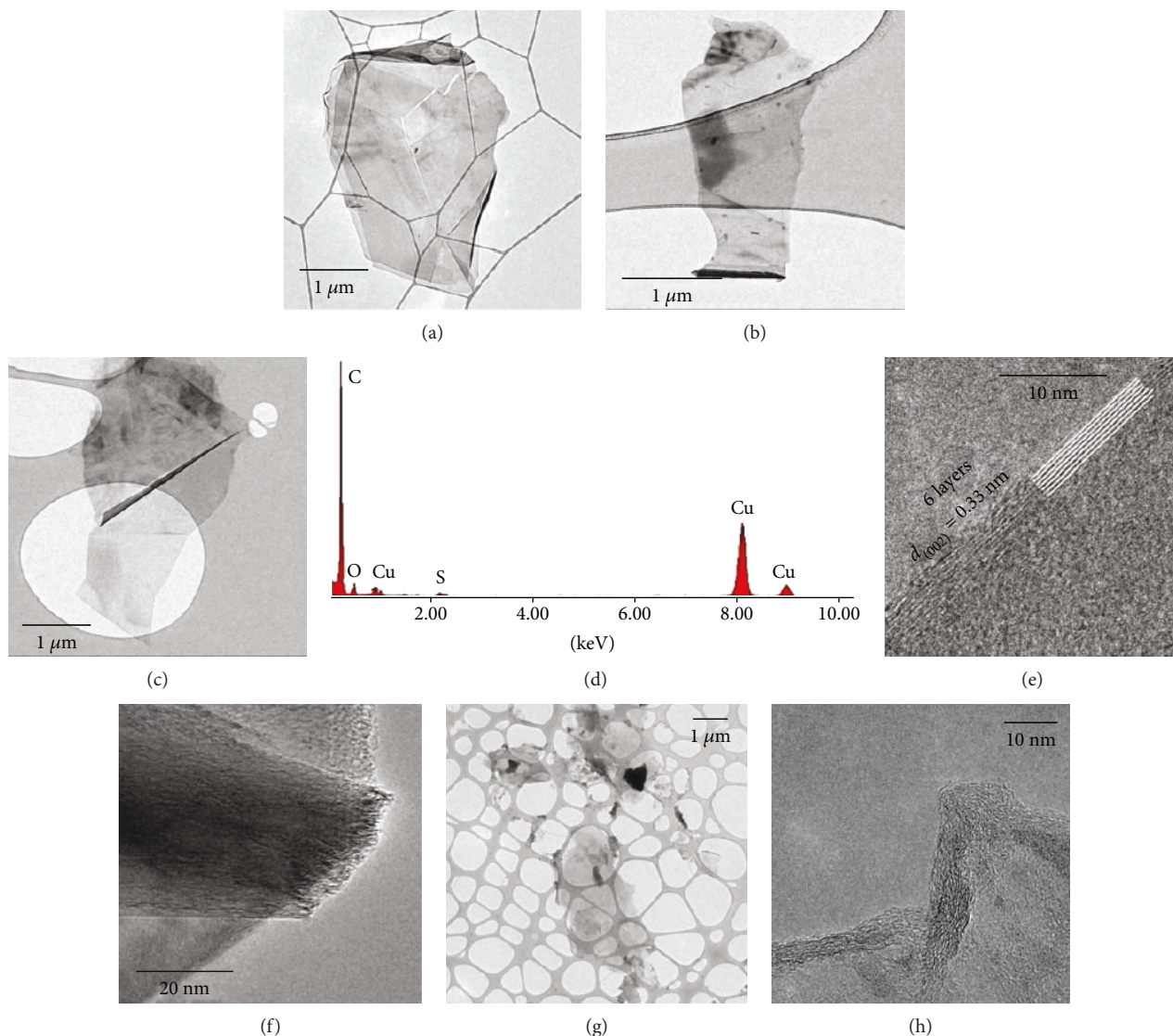


FIGURE 5: TEM images of samples (a) G, (b) GO(F), and (c) RGO(F) obtained by the Fenton method. (d) EDX data for the RGO(F) sample. (e) HRTEM image of the RGO(F) sample. (f) TEM image of the RGO sample obtained without the previous oxidation treatment by the Fenton reaction. (g) TEM image of RGO(H) obtained by Hummers' method. (h) HRTEM image of the RGO(H) sample.

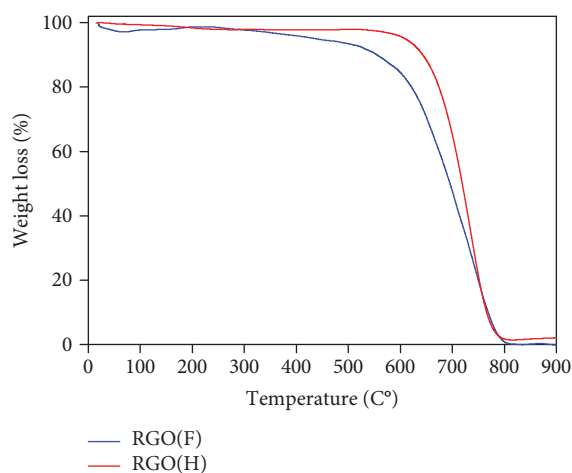


FIGURE 6: TGA profile for the RGO obtained by Fenton's and Hummers' method.

The thermal stability of RGO obtained by Fenton's and Hummers' method using thermogravimetric analysis (TGA) is shown in Figure 6. For both samples, the small mass loss around 100°C is due to the loss of adsorbed water. RGO(F) shows a gradual mass loss from 400 to 800°C due to the oxidation of carbon. For RGO(H), the mass loss takes place from 700 to 800°C, indicating that RGO(H) is thermally more stable than RGO(F) probably due to its higher number of graphene layers. Also, at 800°C the mass loss achieved 100%, confirming that iron was removed entirely from the graphene sheets in the RGO(F) sample.

#### 4. Conclusions

A convenient method for producing a few layers of reduced graphene oxide by the previous oxidation of graphite with a Fenton reagent was demonstrated. The Fenton chemistry takes advantage of the high oxidizing power of hydroxyl

radicals, which can attack the graphene sheets of graphite, thus favoring its exfoliation with ultrasound to obtain a few layers of reduced graphene oxide. The efficiency of graphite delamination was similar to that obtained with Hummers' method, but because the Fenton chemistry oxidizes the edges of graphite preferentially, further chemical reduction with ascorbic acid leads to a synthesis of less defective reduced graphene oxide. Also, the Fenton reagent is environmentally friendlier than other conventional oxidizing agents for this purpose, which makes this method more adequate for large-scale use.

## Data Availability

The data used to support the findings of this study are included within the article.

## Conflicts of Interest

The authors declare that there is no conflict of interest regarding the publication of this paper.

## Acknowledgments

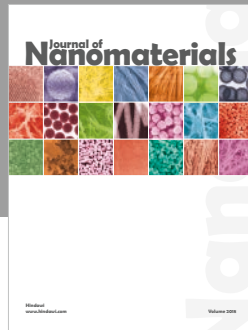
The authors are grateful to FAPEMIG, CNPq, and FINEP for financial support. The Center of Microscopy at the Universidade Federal de Minas Gerais is also acknowledged (<http://www.microscopia.ufmg.br>) for providing the equipment and technical support for experiments involving electron microscopy.

## References

- [1] A. K. Geim and K. S. Novoselov, "The rise of graphene," *Nature Materials*, vol. 6, no. 3, pp. 183–191, 2007.
- [2] A. A. Balandin, "Thermal properties of graphene and nanostructured carbon materials," *Nature Materials*, vol. 10, no. 8, pp. 569–581, 2011.
- [3] A. H. Castro Neto, F. Guinea, N. M. R. Peres, K. S. Novoselov, and A. K. Geim, "The electronic properties of graphene," *Reviews of Modern Physics*, vol. 81, no. 1, pp. 109–162, 2009.
- [4] C. Soldano, A. Mahmood, and E. Dujardin, "Production, properties and potential of graphene," *Carbon*, vol. 48, no. 8, pp. 2127–2150, 2010.
- [5] Q. Han, N. Chen, J. Zhang, and L. Qu, "Graphene/graphitic carbon nitride hybrids for catalysis," *Materials Horizons*, vol. 4, no. 5, pp. 832–850, 2017.
- [6] A. S. Bozzi, R. L. Lavall, T. E. Souza et al., "An effective approach for modifying carbonaceous materials with niobium single sites to improve their catalytic properties," *Dalton Transactions*, vol. 44, no. 46, pp. 19956–19965, 2015.
- [7] D. W. Boukhvalov, Y. W. Son, and R. S. Ruoff, "Water splitting over graphene-based catalysts: ab initio calculations," *ACS Catalysis*, vol. 4, no. 6, pp. 2016–2021, 2014.
- [8] T. A. Saleh, A. Sari, and M. Tuzen, "Effective adsorption of antimony(III) from aqueous solutions by polyamide-graphene composite as a novel adsorbent," *Chemical Engineering Journal*, vol. 307, pp. 230–238, 2017.
- [9] B. Szczeńniak, J. Choma, and M. Jaroniec, "Gas adsorption properties of graphene-based materials," *Advances in Colloid and Interface Science*, vol. 243, pp. 46–59, 2017.
- [10] G. Ersan, O. G. Apul, F. Perreault, and T. Karanfil, "Adsorption of organic contaminants by graphene nanosheets: a review," *Water Research*, vol. 126, pp. 385–398, 2017.
- [11] L. Qu, Y. Liu, J. B. Baek, and L. Dai, "Nitrogen-doped graphene as efficient metal-free electrocatalyst for oxygen reduction in fuel cells," *ACS Nano*, vol. 4, no. 3, pp. 1321–1326, 2010.
- [12] J. Li, Y. Zhang, X. Zhang et al., "S, N dual-doped graphene-like carbon nanosheets as efficient oxygen reduction reaction electrocatalysts," *ACS Applied Materials & Interfaces*, vol. 9, no. 1, pp. 398–405, 2017.
- [13] C. Xu, B. Xu, Y. Gu, Z. Xiong, J. Sun, and X. S. Zhao, "Graphene-based electrodes for electrochemical energy storage," *Energy and Environmental Science*, vol. 6, no. 5, pp. 1388–1414, 2013.
- [14] J. Zhu, D. Yang, Z. Yin, Q. Yan, and H. Zhang, "Graphene and graphene-based materials for energy storage applications," *Small*, vol. 10, no. 17, pp. 3480–3498, 2014.
- [15] J. Mao, J. Iocozzia, J. Huang, K. Meng, Y. Lai, and Z. Lin, "Graphene aerogels for efficient energy storage and conversion," *Energy and Environmental Science*, vol. 11, no. 4, pp. 772–799, 2018.
- [16] G. Gnana Kumar, G. Amala, and S. M. Gowtham, "Recent advancements, key challenges and solutions in non-enzymatic electrochemical glucose sensors based on graphene platforms," *RSC Advances*, vol. 7, no. 59, pp. 36949–36976, 2017.
- [17] A. Nag, A. Mitra, and S. C. Mukhopadhyay, "Graphene and its sensor-based applications: a review," *Sensors and Actuators, A: Physical*, vol. 270, pp. 177–194, 2018.
- [18] S. Stankovich, D. A. Dikin, R. D. Piner et al., "Synthesis of graphene-based nanosheets via chemical reduction of exfoliated graphite oxide," *Carbon*, vol. 45, no. 7, pp. 1558–1565, 2007.
- [19] Y. Zhu, S. Murali, W. Cai et al., "Graphene and graphene oxide: synthesis, properties, and applications," *Advanced Materials*, vol. 22, no. 35, pp. 3906–3924, 2010.
- [20] H. C. Schniepp, J. L. Li, M. J. McAllister et al., "Functionalized single graphene sheets derived from splitting graphite oxide," *Journal of Physical Chemistry B*, vol. 110, no. 17, pp. 8535–8539, 2006.
- [21] R. M. N. M. Rathnayake, H. W. M. A. C. Wijayasinghe, H. M. T. G. A. Pitawala, M. Yoshimura, and H. H. Huang, "Synthesis of graphene oxide and reduced graphene oxide by needle plating natural vein graphite," *Applied Surface Science*, vol. 393, pp. 309–315, 2017.
- [22] X. Ye, Q. Zhou, C. Jia, Z. Tang, Y. Zhu, and Z. Wan, "Producing large-area, foldable graphene paper from graphite oxide suspensions by in-situ chemical reduction process," *Carbon*, vol. 114, pp. 424–434, 2017.
- [23] Z.-J. Fan, W. Kai, J. Yan et al., "Facile synthesis of graphene nanosheets via Fe reduction of exfoliated graphite oxide," *ACS Nano*, vol. 5, no. 1, pp. 191–198, 2011.
- [24] B. Liu, J. Xie, H. Ma et al., "From graphite to graphene oxide and graphene oxide quantum dots," *Small*, vol. 13, no. 18, article 1601001, 2017.
- [25] J. Zhang, Q. Liu, Y. Ruan, S. Lin, K. Wang, and H. Lu, "Monolithic crystalline swelling of graphite oxide: a bridge to ultralarge graphene oxide with high scalability," *Chemistry of Materials*, vol. 30, no. 6, pp. 1888–1897, 2018.

- [26] J. M. Tour, "Top-down versus bottom-up fabrication of graphene-based electronics," *Chemistry of Materials*, vol. 26, no. 1, pp. 163–171, 2014.
- [27] W. S. Hummers Jr and R. E. Offeman, "Preparation of graphitic oxide," *Journal of the American Chemical Society*, vol. 80, no. 6, article 1339, 1958.
- [28] Abid, P. Sehrawat, S. S. Islam, P. Mishra, and S. Ahmad, "Reduced graphene oxide (rGO) based wideband optical sensor and the role of temperature, defect states and quantum efficiency," *Scientific Reports*, vol. 8, no. 1, article 3537, 2018.
- [29] J. Chen, Y. Zhang, M. Zhang et al., "Water-enhanced oxidation of graphite to graphene oxide with controlled species of oxygenated groups," *Chemical Science*, vol. 7, no. 3, pp. 1874–1881, 2016.
- [30] R. Muzyka, M. Kwoka, Ł. Smędowski, N. Díez, and G. Gryglewicz, "Oxidation of graphite by different modified hummers methods," *New Carbon Materials*, vol. 32, no. 1, pp. 15–20, 2017.
- [31] K. Y. Chong, C. H. Chia, S. W. Chook, S. Zakaria, and D. Lucas, "Simplified production of graphene oxide assisted by high shear exfoliation of graphite with controlled oxidation," *New Journal of Chemistry*, vol. 42, no. 6, pp. 4507–4512, 2018.
- [32] S. Chandra, S. Sahu, and P. Pramanik, "A novel synthesis of graphene by dichromate oxidation," *Materials Science and Engineering: B*, vol. 167, no. 3, pp. 133–136, 2010.
- [33] B. C. Brodie, "On the atomic weight of graphite," *Philosophical Transactions of the Royal Society of London*, vol. 149, pp. 249–259, 1859.
- [34] S. Pei and H. M. Cheng, "The reduction of graphene oxide," *Carbon*, vol. 50, no. 9, pp. 3210–3228, 2012.
- [35] K. K. H. De Silva, H. H. Huang, R. K. Joshi, and M. Yoshimura, "Chemical reduction of graphene oxide using green reductants," *Carbon*, vol. 119, pp. 190–199, 2017.
- [36] L. Dong, J. Yang, M. Chhowalla, and K. P. Loh, "Synthesis and reduction of large sized graphene oxide sheets," *Chemical Society Reviews*, vol. 46, no. 23, pp. 7306–7316, 2017.
- [37] N. Agarwal, R. Bhattacharyya, N. K. Tripathi et al., "Derivatization and interlaminar debonding of graphite-iron nanoparticle hybrid interfaces using Fenton chemistry," *Physical Chemistry Chemical Physics*, vol. 19, no. 25, pp. 16329–16336, 2017.
- [38] P. Anastas and N. Eghbali, "Green chemistry: principles and practice," *Chemical Society Reviews*, vol. 39, no. 1, pp. 301–312, 2010.
- [39] H.-K. Jeong, Y. P. Lee, R. J. W. E. Lahaye et al., "Evidence of graphitic AB stacking order of graphite oxides," *Journal of the American Chemical Society*, vol. 130, no. 4, pp. 1362–1366, 2008.
- [40] Z. Q. Li, C. J. Lu, Z. P. Xia, Y. Zhou, and Z. Luo, "X-ray diffraction patterns of graphite and turbostratic carbon," *Carbon*, vol. 45, no. 8, pp. 1686–1695, 2007.
- [41] A. Kaniyoor, T. T. Baby, and S. Ramaprabhu, "Graphene synthesis via hydrogen induced low temperature exfoliation of graphite oxide," *Journal of Materials Chemistry*, vol. 20, no. 39, pp. 8467–8469, 2010.
- [42] L. G. Cançado, A. Jorio, E. H. M. Ferreira et al., "Quantifying defects in graphene via Raman spectroscopy at different excitation energies," *Nano Letters*, vol. 11, no. 8, pp. 3190–3196, 2011.





**Hindawi**  
Submit your manuscripts at  
[www.hindawi.com](http://www.hindawi.com)

